

AD-A022 494

AN EVALUATION OF SOME HIGH STRENGTH TITANIUM ALLOYS
PROCESSED IN HEAVY SECTIONS

Richard Chait, et al

Army Materials and Mechanics Research Center
Watertown, Massachusetts

September 1975

DISTRIBUTED BY:

NTIS

National Technical Information Service
U. S. DEPARTMENT OF COMMERCE

096129

AD



ADA022494

AVSCOM Report No. 76-6 DRSVAV

PRODUCTION ENGINEERING MEASURES PROGRAM
MANUFACTURING METHODS AND TECHNOLOGY

AN EVALUATION OF SOME HIGH STRENGTH TITANIUM ALLOYS PROCESSED IN HEAVY SECTIONS

RICHARD CHAIT and THOMAS S. DeSISTO
Army Materials and Mechanics Research Center
Watertown, Massachusetts 02172

AMMRC PTR 75-3

September 1975

Final Report

DDC
RECEIVED
MAR 31 1976
C

Approved for public release; distribution unlimited.

Prepared for

U.S. ARMY AVIATION SYSTEMS COMMAND
St. Louis, Missouri 63166

REPRODUCED BY
NATIONAL TECHNICAL
INFORMATION SERVICE
U. S. DEPARTMENT OF COMMERCE
SPRINGFIELD, VA. 22161

ACCESSION for	
NTIS	White Section <input checked="" type="checkbox"/>
DOC	Red Section <input type="checkbox"/>
UNANNOUNCED JUSTIFICATION	<input type="checkbox"/>
BY.....	
DISTRIBUTION/AVAILABILITY CODES	
NO.	AVAIL. and/or SPECIAL
A	

The findings in this report are not to be construed as an official Department of the Army position, unless so designated by other authorized documents.

Mention of any trade names or manufacturers in this report shall not be construed as advertising nor as an official indorsement or approval of such products or companies by the United States Government.

DISPOSITION INSTRUCTIONS

Destroy this report when it is no longer needed.
Do not return it to the originator.

UNCLASSIFIED

SECURITY CLASSIFICATION OF THIS PAGE (When Data Entered)

REPORT DOCUMENTATION PAGE		READ INSTRUCTIONS BEFORE COMPLETING FORM
1. REPORT NUMBER AVSCOM Report No. 76-6 DRSVAV	2. GOVT ACCESSION NO.	3. RECIPIENT'S CATALOG NUMBER
4. TITLE (and Subtitle) AN EVALUATION OF SOME HIGH STRENGTH TITANIUM ALLOYS PROCESSED IN HEAVY SECTIONS	5. TYPE OF REPORT & PERIOD COVERED Final Report	
	6. PERFORMING ORG. REPORT NUMBER AMMRC PTR 75-3	
7. AUTHOR(s) Richard Chait and Thomas S. DeSisto	8. CONTRACT OR GRANT NUMBER(s)	
9. PERFORMING ORGANIZATION NAME AND ADDRESS Army Materials and Mechanics Research Center Watertown, Massachusetts 02172 DRXMR-L	10. PROGRAM ELEMENT, PROJECT, TASK AREA & WORK UNIT NUMBERS D/A Project: 1736039 PEMA AMCMS Code: 4097.94.2.P6039 (XL2)	
11. CONTROLLING OFFICE NAME AND ADDRESS U.S. Army Aviation Systems Command ATTN: DRSVAV-EXT P.O. Box 209, St. Louis, Missouri 63166	12. REPORT DATE September 1975	
	13. NUMBER OF PAGES 22	
14. MONITORING AGENCY NAME & ADDRESS (if different from Controlling Office)	15. SECURITY CLASS. (of this report) Unclassified	
	15a. DECLASSIFICATION/DOWNGRADING SCHEDULE	
16. DISTRIBUTION STATEMENT (of this Report) Approved for public release; distribution unlimited.		
17. DISTRIBUTION STATEMENT (of the abstract entered in Block 20, if different from Report)		
18. SUPPLEMENTARY NOTES		
19. KEY WORDS (Continue on reverse side if necessary and identify by block number) Titanium alloys Extrusion Microstructure Heat treatment Fabrication Mechanical properties		
20. ABSTRACT (Continue on reverse side if necessary and identify by block number) (SEE REVERSE SIDE)		

UNCLASSIFIED

SECURITY CLASSIFICATION OF THIS PAGE(When Data Entered)

Block No. 20

ABSTRACT

Utilization of advanced titanium alloys in heavy sections depends to a large extent on the ability to fabricate these sections. This study is concerned with the high strength alpha-beta alloy Ti-6Al-6V-2Sn (Ti-662) and the metastable beta alloy Ti-8Mo-8V-2Fe-3Al (Ti-8823) and their fabrication in large sections. The extrusion technique utilized to achieve better than a 6:1 reduction ratio for a heavy section cylindrical hollow of this alloy is described. Following extrusion, the alloys were given one of two heat treatments: for the Ti-662 the solutionize and age or solutionize and overage heat treatments; for the Ti-8823 alloy the commonly suggested solutionize and age heat treatment or a direct age without the intermediate solutionize. The influence of these heat treatments is given in terms of microstructure and mechanical properties (yield strength, tensile strength, elongation, reduction of area, and fracture toughness). Test specimens taken at the outer diameter (OD), midwall (MW), and inner diameter (ID) in the longitudinal and transverse directions provide information on orientation and thickness effects.

UNCLASSIFIED

SECURITY CLASSIFICATION OF THIS PAGE(When Data Entered)

FOREWORD

This project was accomplished as part of the US Army Aviation Systems Command Manufacturing Technology program. The primary objective of this program is to develop, on a timely basis, manufacturing processes, techniques, and equipment for use in production of Army materiel. Comments are solicited on the potential utilization of the information contained herein as applied to present and/or future production programs. Such comments should be sent to: US Army Aviation Systems Command, ATTN: DRSAV-EXT, P.O. Box 209, St. Louis, MO 63166.

The extrusion of the heavy section titanium alloys for helicopter components, such as main rotor driveshafts and rotor blade spars, is the subject of this report. The extrusion operation was performed by Cameron Iron Works, Houston, Texas, under contract DAAG46-71-C-0058. The cooperation of those at Cameron who were involved in this program is appreciated. In particular, the assistance of Mr. Colin Stead is acknowledged.

CONTENTS

	Page
FOREWORD.	iii
INTRODUCTION.	1
MATERIALS AND PROCESSING HISTORY.	2
MECHANICAL TESTING PROCEDURE.	7
EVALUATION OF MECHANICAL BEHAVIOR	
Ti-662 Alloy	8
Ti-8823 Alloy.	10
DISCUSSION.	12
SUMMARY AND CONCLUSIONS	15
A. Ti-662	15
B. Ti-8823.	18

INTRODUCTION

Using high strength titanium alloys in large section components of Army aircraft has the potential of improving performance because of attractive strength: weight ratios. However, the ability to utilize advanced high strength titanium alloys in heavy section applications depends on improved processing techniques as well as an understanding of the effect that these processing techniques have on microstructure and subsequent mechanical properties.

This report focuses on the fabrication of an alpha-beta alloy Ti-6Al-6V-2Sn (Ti-662) and a metastable beta alloy Ti-8Mo-8V-2Fe-3Al (Ti-8823). The Ti-662 alloy is capable of achieving high strength levels; however, as shown in Figure 1, this alloy is unable to maintain these levels as the section size is increased.¹⁻³

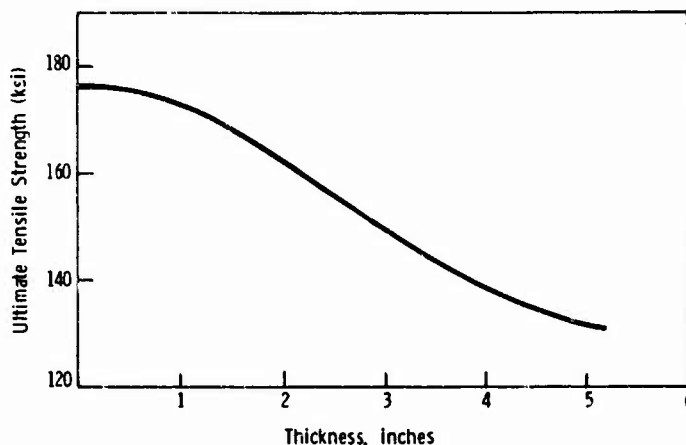


Figure 1. Through-the-Thickness Strength of Ti-662.
Data Replotted from Reference 1.

The metastable beta alloy Ti-8823 was developed by the Army⁴ with an eye toward heavy section application. As with all metastable beta alloys, the retention of the beta phase at room temperature makes possible the capacity for through-hardening of thick sections upon aging. As a result, through-the-section strength properties are more uniform when compared to those obtained from equal section sizes of alpha-beta alloys.¹ In addition, attractive strength values accompanied by excellent fracture toughness are possible. Average values of 177 ksi yield strength and 181 ksi tensile strength were recently obtained⁵ in the longitudinal direction through a 3-inch section. This strength level was accompanied by excellent fracture toughness levels that averaged 51.5 ksi $\sqrt{\text{inch}}$. However, a very coarse beta grain size is believed to be the cause of the low ductility values observed (average reduction of area value of 3.3%).

1. HEIL, W. H. *New Developments in High Strength Titanium Alloys*. Titanium Course, New York University, September 1969.
2. HICKEY, C. F. *Effect of Microstructure and Cooling Rate on the Mechanical Properties of Ti-6Al-6V-2Sn*. Army Materials and Mechanics Research Center, AMRA TR 65-16, July 1965.
3. HICKEY, C. F., and FOPIANO, P. I. *Some Observations on the Hardenability of Ti-6Al-6V-2Sn*. *Met. Trans.*, June 1970 p. 1775.
4. HUNTER, D. B. *Metastable Beta Sheet Alloy Ti-8Mo-8V-2Fe-3Al*. Army Materials and Mechanics Research Center, WAL TR 40S/2-14, October 1966.
5. CHAIT, R., and DeSISTO, T. S. *The Fracture Toughness of Three Heavy Section Titanium Alloys*. Army Materials and Mechanics Research Center, AMMRC PTR 72-5, October 1972.

There have been attempts to improve hot working practices of large sections with the goal of reducing the grain size. For example, material receiving over 90% reduction as it was pressed, upset, and forged in various stages from an ingot to an 8-1/2-inch round has been processed.⁶ With this amount of working relatively coarse grain sizes of ASTM 0 to 2 persisted and, as a result, the desired ductility levels were not achieved. As noted by Bohanek,⁶ continuous hot working at sufficient reduction is required to reduce the grain size of large section products to a level where improved ductility will be realized. While smaller grain sizes (ASTM 5 to 6) have resulted from a high reduction extrusion that produced a hollow cylinder having a 2-inch outer diameter (OD) and 1/4-inch wall,⁷ much larger extruded sections with significant amounts of hot work have not been evaluated. Increased amounts of hot working are also expected to benefit the Ti-662 alloy since a finer equiaxed alpha particle size is associated with improved fracture toughness.⁵ In the present report the details of extruding a heavy section, hollow cylinder of both Ti-662 and Ti-8823 alloys are presented. The mechanical properties are detailed and discussed in terms of the resulting microstructure.

MATERIALS AND PROCESSING HISTORY

The Ti-662 and Ti-8823 alloys of concern in this investigation were melted by Titanium Metals Corporation of America (TMCA). The alloys have the chemical composition shown in Table 1. As shown in the processing overview of Figure 2, the billets were reduced from 28 inches in diameter to 20 inches in diameter by TMCA prior to extrusion. The extrusion portion of the processing was performed by Cameron Iron Works, Houston, Texas, with a 20,000-ton press utilizing the method shown schematically in Figure 3. Billet location on the press before, during, and after extrusion are shown in the photographs of Figure 4. Note that with the die and container moving, the end result is similar to that obtained with the direct extrusion process shown in Figure 5.

For extrusion of the Ti-662 alloy, a temperature of 1625 F was selected to reduce the possibility of beta flecks appearing in the microstructure.* These flecks are chemical gradients of iron and copper* and appear to be detrimental to fracture toughness.⁵ The Ti-8823 alloy was extruded at 1700 F. It was hoped that at this temperature sufficient work would be introduced into the material to effect recrystallization without significant grain growth. From available elevated temperature flow stress data⁸ shown in Figure 6, it was determined that an extrusion temperature of 1700 F was feasible. Additional processing details for each alloy are shown in Table 2. Performing the extrusion as outlined above it was possible to effect an 84% reduction (6.3:1 reduction ratio). The product of this process was a cylindrical hollow, about 7 feet long, having the approximate dimensions of 11-3/8 inches OD and 3-1/8 inches wall thickness. This massive section precluded

*RUSSELL, H. A., Titanium Metals Corporation of America, private communication, July 1969.

6. BOHANEK, E. *Evaluation of Several Commercial Heats of Ti-8Mo-8V-2Fe-3Al*. Titanium Metals Corporation of America, Mechanical Report No. 45, August 1970.
7. BOHANEK, E. *Extrusion and Processing of Ti-3Al-2.5V and Ti-8Mo-8V-2Fe-3Al Tube Hollows*. Titanium Metals Corporation of America, Technical Report No. 18, February 1972.
8. DOUGLAS, J. R., and ALTAN, T. *A Study of Mechanics of Closed-Die Forgings, Phase II*. Battelle Memorial Institute, Contract DAAG-46-71-C-0095, Final Report, AMMRC CTR 72-25, November 1972.

Table 1. COMPOSITION

Alloy	Element (Weight Percent)									
	Al	V	Mo	Fe	Sn	Cu	C	O	H	N
Ti-6Al-6V-2Sn (Ti-662)	5.58	5.67	-	0.72	2.01	0.57	0.024	0.14	0.006	0.015
Ti-8Mo-8V-2Fe-3Al (Ti-8823)	3.08	8.08	7.80	2.07	-	-	0.035	0.133	0.006	0.010

Table 2. PROCESSING PROCEDURE

Ti-662	Ti-8823
1. Preheat 1500 F - 5-1/4 Hr	1. Preheat 1500 F - 6 Hr
2. Soak 1625 F - 3 Hr	2. Soak 1700 F - 5-3/4 Hr
3. Transfer to Press - 30 Sec	3. Transfer to Press - 30 Sec
4. Extrude	4. Extrude
5. Air Cool	5. Air Cool
6. Heat Treat	6. Heat Treat

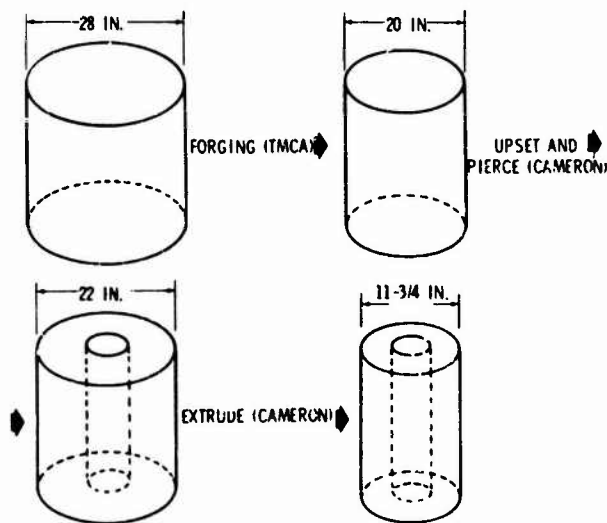


Figure 2. Review of Processing up to the Point of Extrusion.

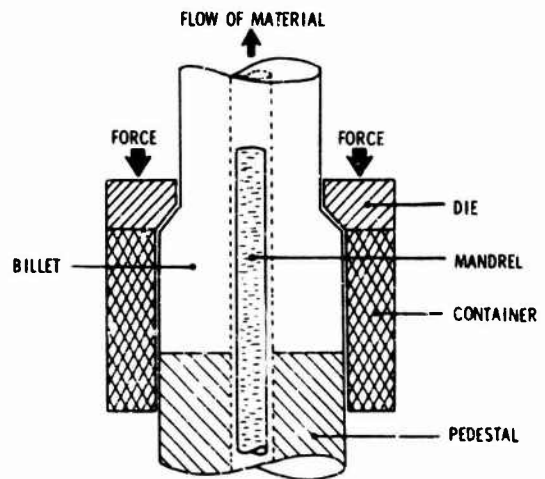
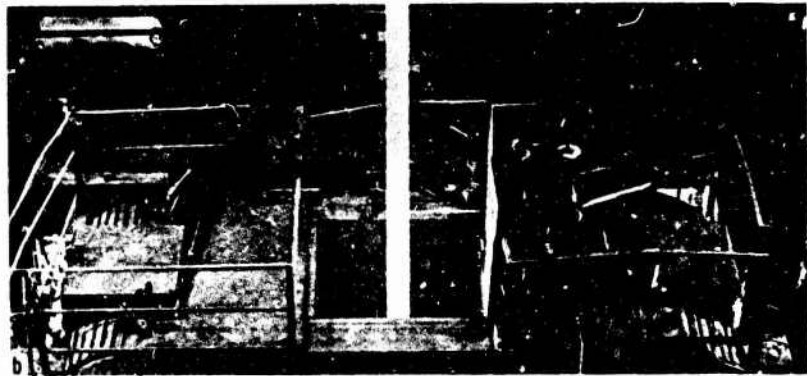


Figure 3. Schematic of Extrusion Process.



19-066-713/AMC-74



19-066-714/AMC-74



19-066-83/AMC-72

Figure 4. Location of Billet During Extrusion Operation. a. Billet Being Placed on Pedestal, b. Extruded Billet Coming thru Top Crosshead and, c. Removal of Billet from Press. (Courtesy of Cameron Iron Works)

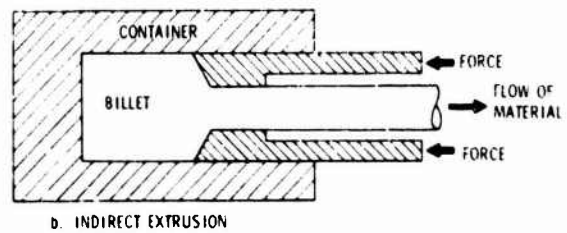
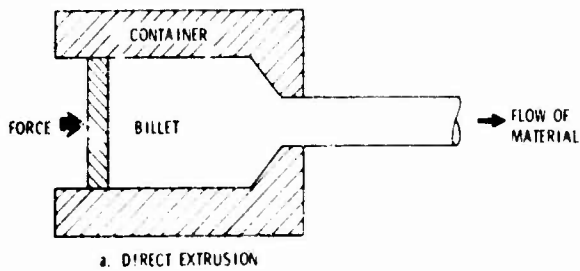


Figure 5. Basic Types of Extrusion.

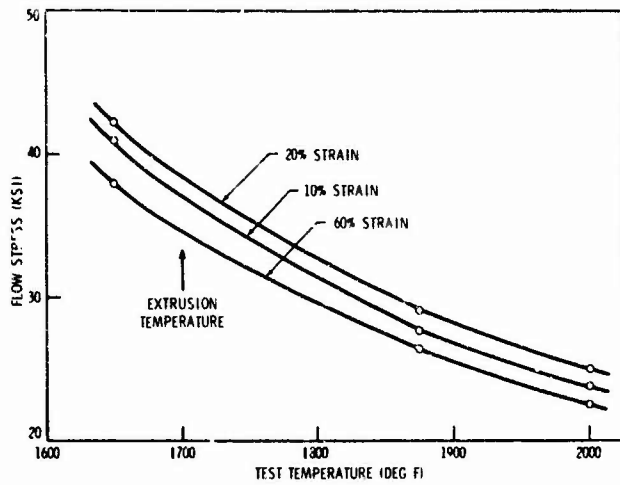
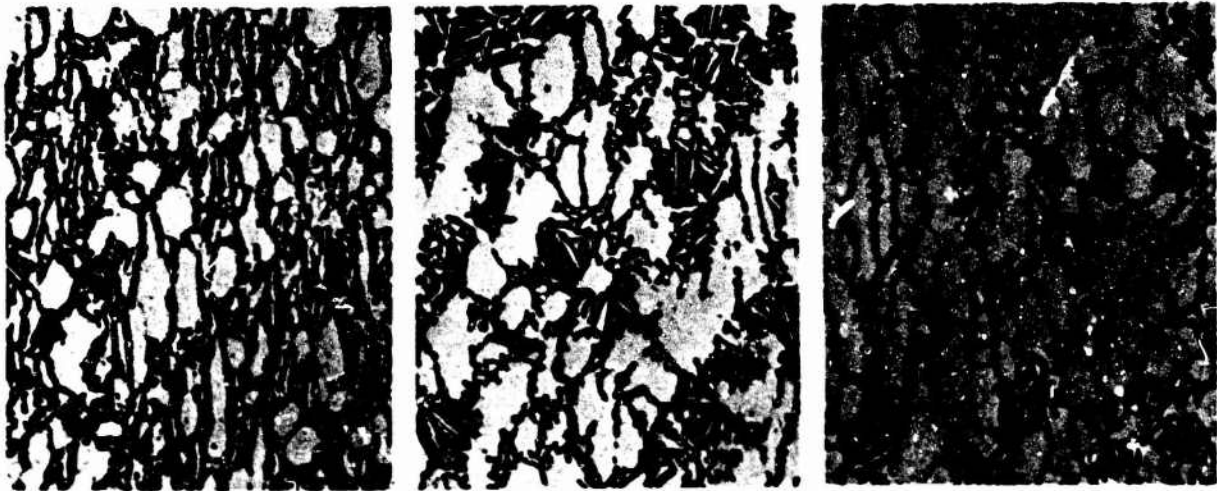


Figure 6. Isothermal Compressive Flow Stress of Ti-8823 as a Function of Test Temperature. Data Replotted from Reference 8.

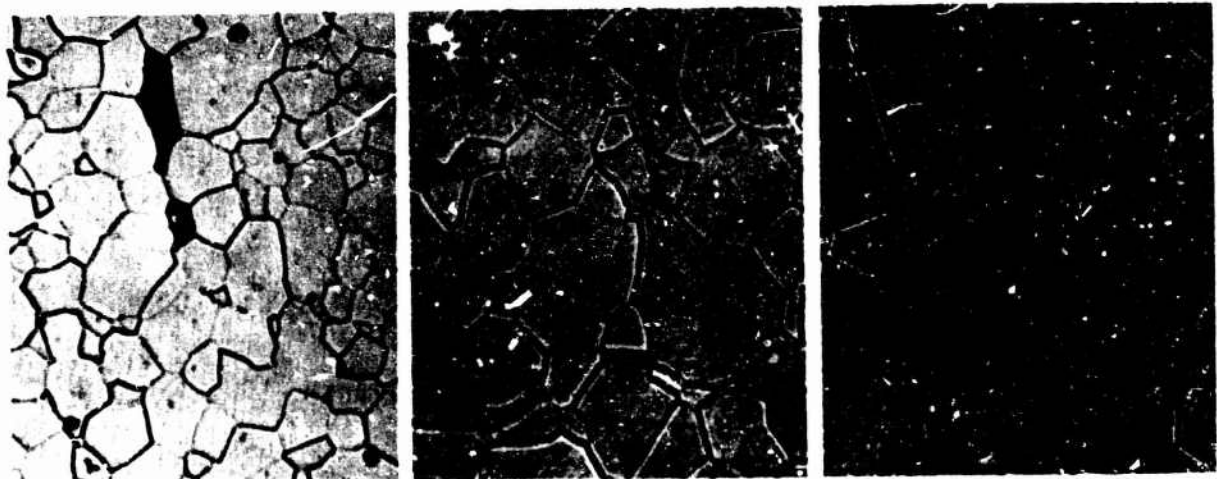


OD

MW

ID

Figure 7. As-Extruded Microstructure of Ti-662 at OD, MW, and ID Locations. Mag. 500X



OD

MW

ID

Figure 8. As-Extruded Microstructure of Ti-8823 at OD, MW, and ID Locations. Areas at OD Location that Appear Dark are Unrecrystallized Regions. Mag. 100X

a water quench after extrusion. The resulting as-extruded microstructures are shown in Figure 7 for Ti-662 and Figure 8 for Ti-8823. The ASTM grain size for the as-extruded microstructure of the Ti-8823 alloy was 3 to 5, a considerable improvement in grain size over like sections that have received less concentrated mechanical working^{5,6} (cf. Figures 8 and 20, the latter to be the subject of discussion in another section). However, at the outerwall location there were regions of unrecrystallized beta. The unrecrystallized microstructure of higher magnification is shown in Figure 9. Note the appearance of equiaxed grains that are beginning to form from the large unrecrystallized beta grains. For the Ti-662 alloy, the combination of the 1625 F extrusion temperature and heavy mechanical working results in a fine alpha particle size as shown in Figure 7.

Following extrusion, the as-received billet was cut into 2-1/2-foot lengths for heat treatment. Two heat treatments were selected for each alloy. For the Ti-662 these were 1) the solutionizing and aging (STA) heat treatment, and 2) the solutionizing and overaging (STOA) heat treatment. The two choices for the Ti-8823 were 1) the generally recommended STA heat treatment, and 2) the direct aging (DA) heat treatment. The DA heat treatment was selected in an attempt to evaluate response of Ti-8823 to this heat treatment and effect a higher strength without a sacrifice in toughness or ductility. Temperatures and times for these heat treatments are detailed in Table 3. It is of interest to note that quenching from the solutionizing temperatures was accomplished in 10 seconds or less utilizing a roll-out furnace. The microstructure of the heat-treated Ti-662 is shown in Figure 10.



Figure 9. Unrecrystallized Region in As-Extruded Microstructure of Ti-8823.
Note Emergence of Equiaxed Grains from Region. Mag. 500X

Table 3. HEAT TREATMENT

Alloy	Condition	Solutionizing Temperature and Time Prior to WQ	Aging Temperature and Time Prior to AC
Ti-662*	STA	1600 F - 3 Hr	1000 F - 4 Hr
	STOA	1600 F - 3 Hr	1300 F - 6 Hr
Ti-8823†	STA	1475 F - 1-1/2 Hr	1000 F - 8 Hr
	DA		950 F - 8 Hr

*Extrusion Temperature - 1625 F

†Extrusion Temperature - 1700 F

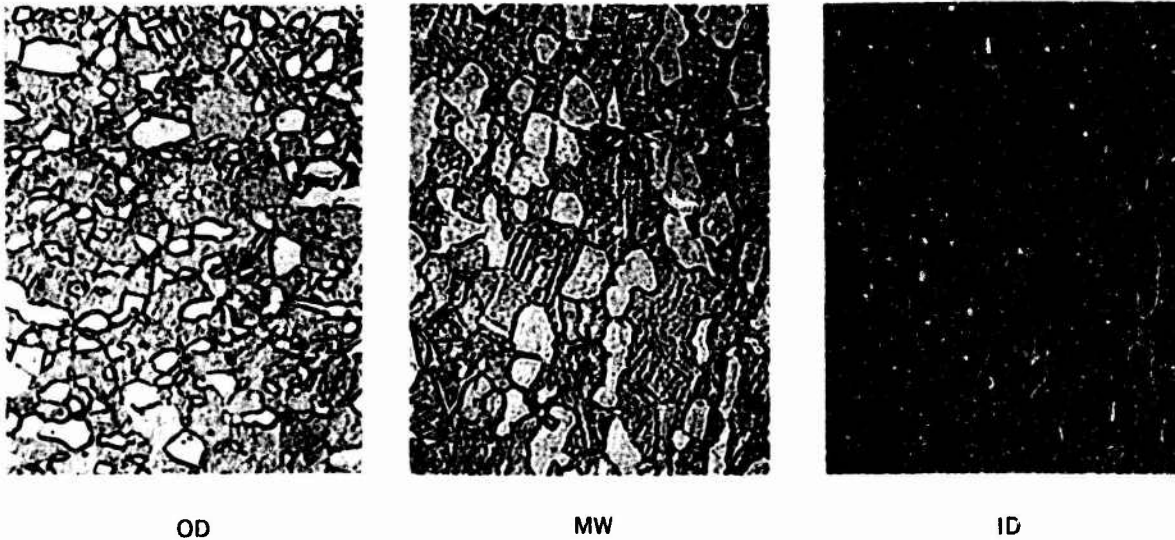


Figure 10. Microstructure of Ti-662 (STA) at OD, MW, and ID Locations. Mag. 500X

MECHANICAL TESTING PROCEDURE

Cylindrical tension specimens (0.252-in. diameter) were taken from the heat-treated sections in both the longitudinal and transverse directions, from the OD, midwall (MW), and inner diameter (ID) locations. Standard Charpy toughness specimens were machined in an identical manner. According to recent ASTM definitions,⁹ the longitudinal direction corresponds to the LR orientation and the transverse to the CR orientation.

The tension tests were performed on a 120,000-lb capacity universal hydraulic testing machine at a platen displacement of 0.005 in./min. The Charpy specimens were precracked in a ManLabs Model FCM-300B machine and tested to failure in three-point bending to determine an approximate plane strain fracture toughness condition designated K_{Ic} . The precracking procedure involved initiation of the crack in compression and subsequent growth in tension, a method which gave uniform crack fronts for high strength steels as well as titanium alloys.¹⁰ Transverse compact

9. *Standard F-399-72*. Annual Book of ASTM Standards, Part 31, American Society for Testing and Materials, Philadelphia, PA, 1973.

10. ROLLINS, K. A., CHAIT, R., and LUM, P. T. *On the Precracking Procedure for Fracture Toughness Determination*. Army Materials and Mechanics Research Center, AMMRC TN 72-24, September 1972.

tension specimens (CR orientation) were machined for plane strain K_{IC} fracture toughness determination. The initial portion of the crack was located at the MW and propagated toward the ID location. Precracking of the compact tension specimen was performed on a 20,000-lb capacity MTS closed loop hydraulic test system and tested to failure in a 10,000-lb Instron tension machine. All precracking and testing procedure with the exception of the crack-front profile conformed to current ASTM Standards³ Although it is felt that these data are valid and should be reported as valid K_{IC} plane strain fracture toughness values, the difference between any two of the crack length measurements exceeds the allowable limit given in the ASTM Standard.

EVALUATION OF MECHANICAL BEHAVIOR

Ti-662 Alloy

Tensile properties for Ti-662 alloy in both the STA and STOA conditions are shown in Figure 11. Exact values are given in Table 4. As expected in the STA condition, both yield strength and ultimate tensile strength are maximum at the OD and ID locations where the fastest cooling rates are obtained. For example, there is about a 20 ksi decrease in the yield strength and ultimate tensile strength as one progresses from OD to the MW locations. The lower strength at the MW is accompanied by a slight increase in the elongation. However, reduction of area at the midwall is greater than the ID but approximately the same as at the OD location. In the overaged condition the strength properties are lower but uniform through the section. Ductility values in the STOA condition are about double that for the STA condition.

For both STA and STOA conditions, the transverse orientation generally leads to slightly higher strength than the longitudinal orientation. The reverse is true for the ductility values. The notch strength of both the STA and STOA materials was fairly uniform across the section as shown in Figure 12. Larger notch strengths were noted for the STOA materials because of the increase in ductility.

Fracture toughness values at the various locations were obtained with precracked Charpy specimens tested in slow bend. For the STA material, the K_Q values

Table 4. ROOM TEMPERATURE TENSILE PROPERTIES

Alloy	H. T.	Orientation	0.2% Yield Strength ksi			Tensile Strength ksi			Elongation %			Reduction of Area %		
			OD	MW	ID	OD	MW	ID	OD	MW	ID	OD	MW	ID
Ti-662	STA	L	180.0	159.9	172.1	191.0	172.9	186.4	9.8	13.9	9.0	25.2	27.1	22.4
		T	176.9	161.3	182.5	188.8	173.8	193.2	9.0	13.5	7.0	21.7	21.4	12.4
	STOA	L	147.3	142.9	145.9	159.6	156.5	159.5	21.3	21.0	20.0	41.9	38.3	38.9
		T	149.3	147.9	148.3	158.0	156.6	161.4	18.5	20.8	19.0	41.5	37.9	34.3
Ti-8823	DA	L	173.8	177.2	176.7	190.5	194.2	190.8	9.8	6.0	8.0	14.2	7.6	10.0
		T	184.2	184.8	183.9	196.4	196.2	196.2	5.0	6.3	6.0	6.9	10.3	8.4
	STA	L	160.0	175.1	179.5	175.8	184.5	185.6	9.3	3.7	3.0	14.0	5.5	4.0
		T	168.9	184.2	178.1	181.5	190.2	186.1	4.0	3.0	4.0	5.1	4.9	6.5

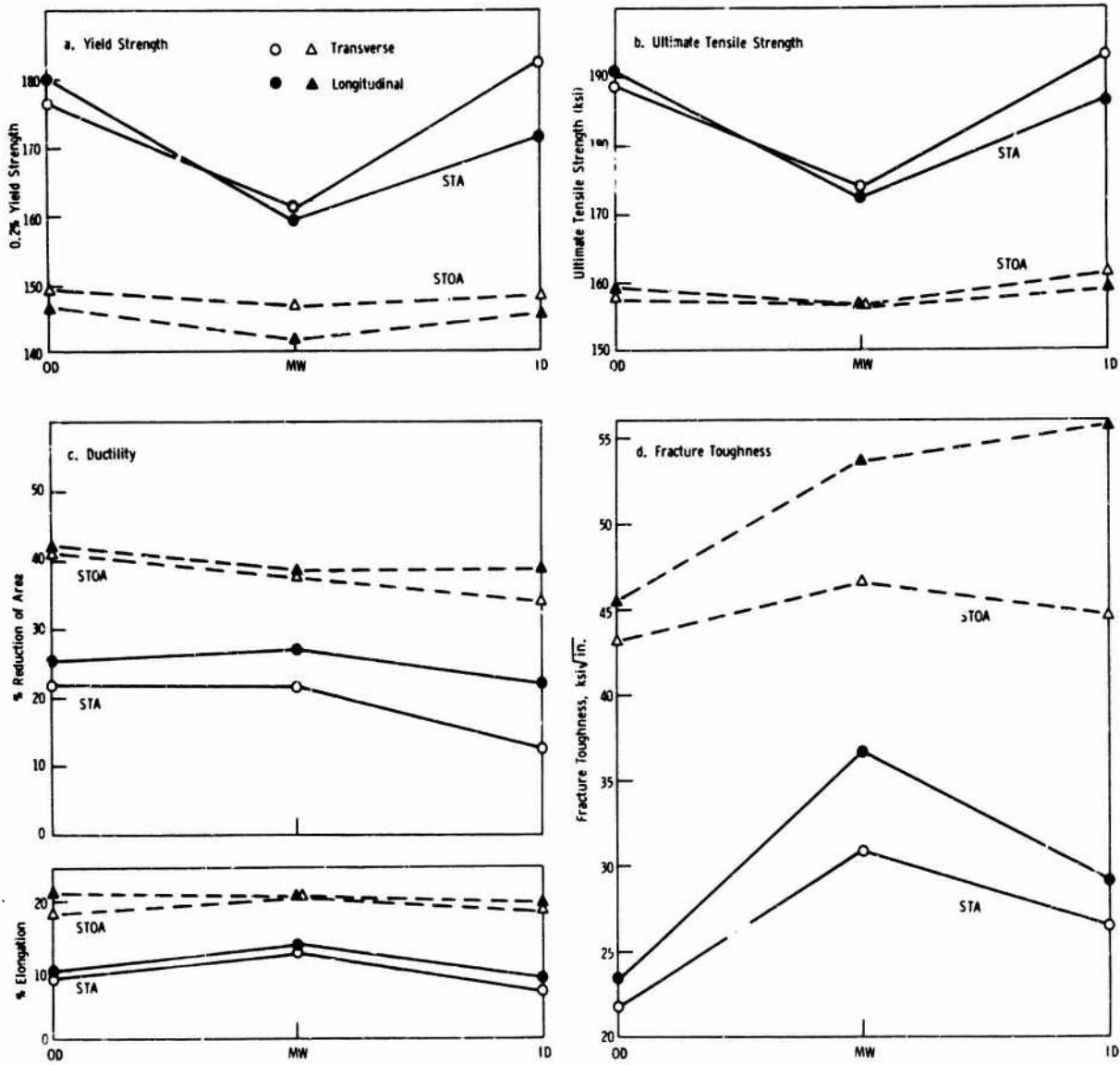


Figure 11. Strength, Ductility, and Toughness Properties of Ti-662 as Influenced by Heat Treatment, Orientation, and Location.

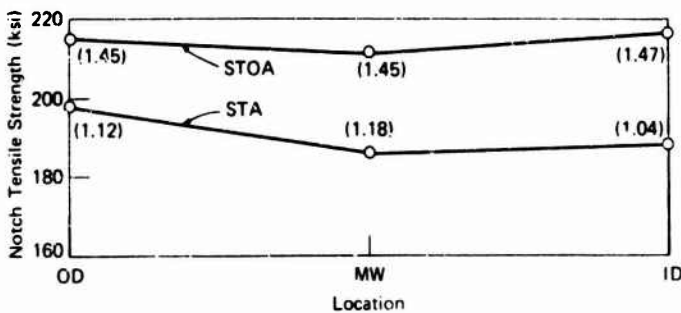


Figure 12. Notch Tensile Strength ($K_t=4.0$) of Ti-662 in Transverse Orientation as Influenced by Heat Treatment and Location. Notch Strength Ratios are Shown in Parenthesis.

are maximum at the MW where lower strength was observed. Specimens oriented longitudinally led to the highest toughness value. The same is true for the material in the STOA condition. However, it should be noted that the fracture toughness of the STOA material exhibited through-the-thickness uniformity for the transverse orientation only.

Ti-8823 Alloy

A summary of the tension test results is shown in Table 4 for both DA and STA materials. Discussing the STA material first, it is seen in Figure 13 that location, i.e., OD, MW, or ID, has a profound effect on the strength level. The 0.2% offset yield strength σ_{ys} and ultimate tensile strength σ_{uts} values obtained at the OD were lower than at the MW or ID locations. In the longitudinal direction, σ_{ys} (σ_{uts} values in parenthesis) = 160 (176) ksi at the OD, while at the MW and ID σ_{ys} = 175 (184) ksi and 179 (186) ksi, respectively. The transverse strength values were about 5 to 10 ksi higher for both σ_{ys} and σ_{uts} except at the ID where there was no effect of orientation. Lower strength values at the OD were accompanied by an elongation of 9% and reduction of area (RA) of about 14%. Transverse ductility values were markedly lower at the OD location only. Notch tensile properties reflect the variation in mechanical properties as shown in Figure 14, i.e., the notch sensitivity is less at the OD than at the MW or ID. This is also seen in terms of the notch strength ratio values (NSR) shown in parentheses in the figure. At the OD, NSR = 0.97 while at the MW and ID, NSR = 0.75 to 0.80.

While the STA material exhibited considerable variation in strength through-the-thickness, the response of the material to DA was such that strength level was independent of location, as shown in Figure 13. Longitudinal σ_{ys} remained at about 175 ksi and σ_{uts} at 190 ksi levels for the OD, MW, and ID locations. Transverse strength values were about 5 to 10 ksi higher but again were uniform throughout the section. The greatest difference in strength between the STA and DA materials occurs at the OD where there was about a 15 ksi difference in σ_{ys} and σ_{uts} values both in the longitudinal and transverse directions. While the σ_{ys} values of the STA material at the MW and ID locations were comparable to that of DA material, there were significant differences in σ_{uts} values. The larger σ_{uts} values of the DA material at these locations is probably due to a greater degree of strain hardening. The strain hardening exponent n in the power law expression $\sigma = Ke^n$ relating true stress to true strain was determined for both STA and DA materials at the MW and ID locations. These calculations showed the DA material to have the greater degree of strain hardening ($n_{DA}=0.05$, $n_{STA}=0.03$).

Ductility values were not degraded as a result of the generally higher strength levels of the DA material. The RA and elongation at the OD were about the same for the STA and DA materials despite a difference of 13 ksi in σ_{ys} and 15 ksi in σ_{uts} . In the longitudinal direction ductility values at the OD location were approximately 14% for the RA and 10% for the elongation. The transverse ductility values at the OD were considerably lower. At the MW and ID the RA and elongation, without regard to orientation, leveled off to about 7 to 10% and 6 to 8%, respectively. Note at the MW the transverse ductility of the DA material is greater than the longitudinal ductility. However, in both instances, the ductility for the DA material is greater than that of the STA material.

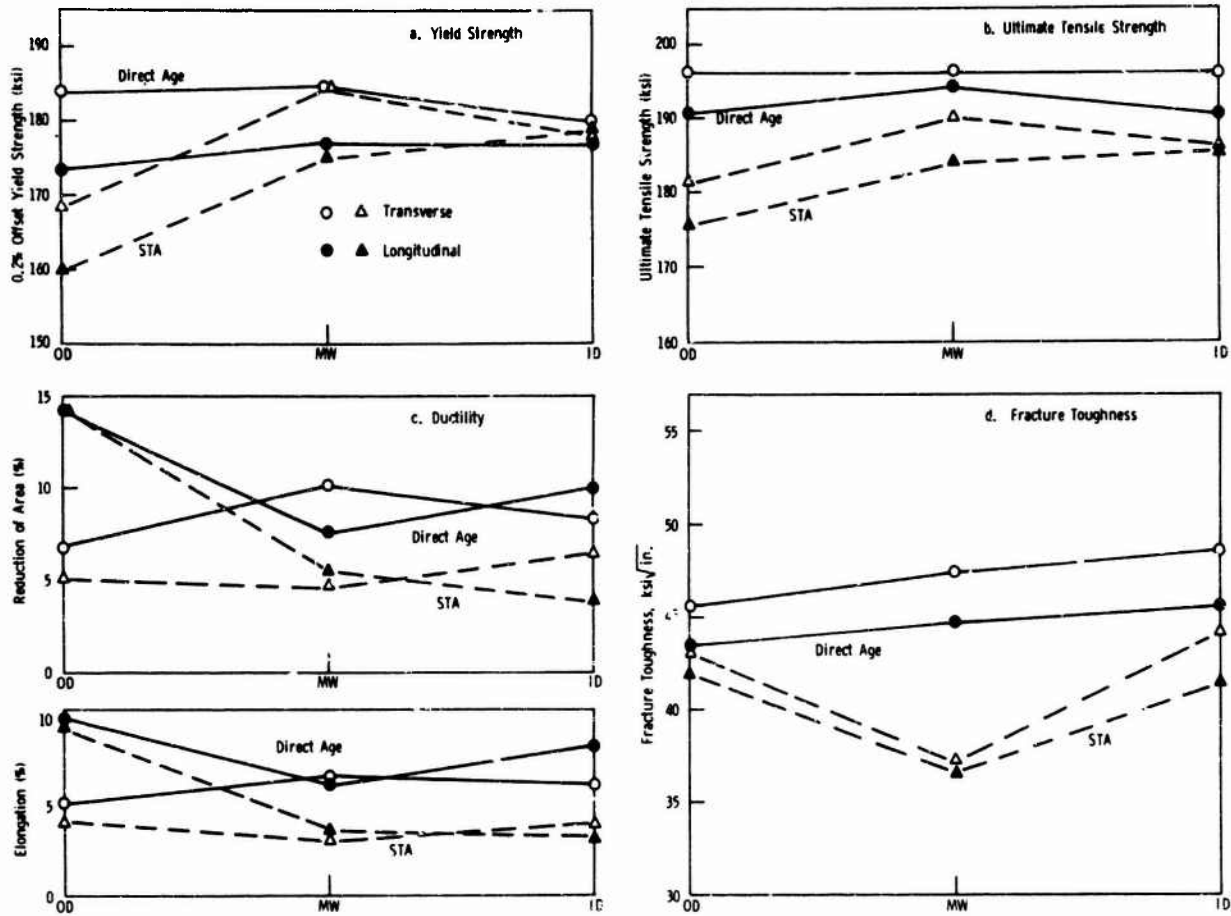


Figure 13. Strength, Ductility, and Toughness Properties of Ti-8823 as Influenced by Heat Treatment, Orientation, and Location.

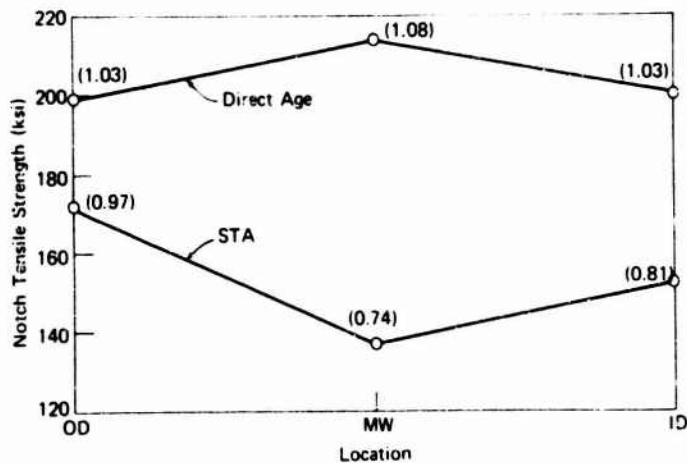


Figure 14. Notch Tensile Strength ($K_t=4.0$) of Ti-8823 in Transverse Orientation as Influenced by Heat Treatment and Location. Notch Strength Ratios are Shown in Parenthesis.

Notch tensile properties of the DA material also reflects uniform strength levels through the thickness. As shown in Figure 14, the notch strength is between 200 to 210 ksi for the three locations. This corresponds to an NSR = 1.03 to 1.08, considerably above that for the STA material.

As with the tensile properties, the fracture toughness of the DA material is superior to that of the STA material. As shown in Figure 13, K_Q does not change significantly with through-the-thickness location for the DA material. On the other hand, a sharp dip is seen in K_Q at the MW for the STA material. Plane strain fracture toughness values obtained from MW compact tension specimens served to check the validity of the K_Q values obtained from precracked Charpy specimens. For DA material, $K_{IC} = 49.9 \text{ ksi}\sqrt{\text{in.}}$, while from the precracked Charpy specimens $K_Q = 47.4 \text{ ksi}\sqrt{\text{in.}}$. The STA material showed similar agreement ($K_{IC} = 39.3 \text{ ksi}\sqrt{\text{in.}}$, $K_Q = 36.7 \text{ ksi}\sqrt{\text{in.}}$). The excellent agreement stemmed from the fact that in all cases the thickness requirement⁹ of $2.5 (K_{IC}/\sigma_{ys})^2$ was met.

Precracked Charpy specimens, loaded in three-point bending, were also utilized to determine K_{ISCC} in 3.5% NaCl for both the STA and DA materials. Two locations were selected for comparison, MW and ID. The DA material exhibited K_{ISCC} of $25.7 \text{ ksi}\sqrt{\text{in.}}$ at the MW and $26.7 \text{ ksi}\sqrt{\text{in.}}$ at the ID. For the STA material, $K_{ISCC} = 16.0 \text{ ksi}\sqrt{\text{in.}}$ for the MW and $12.5 \text{ ksi}\sqrt{\text{in.}}$ for the ID.

DISCUSSION

The first stage of hardening during aging of Ti-662 has been associated with the decomposition of the martensite (that forms as a result of the quench from the solutionizing temperature) to alpha and beta.¹¹ Since the cooling rate is lowest at the MW it is not unexpected that the strengthening at the MW location is less than at the OD or ID. At the MW location the strength level that is obtained as a result of STA heat treatment agrees well with that predicted from Figure 1 for the same thickness. Also, it is interesting to note that the temperatures used in the processing and heat treatment of Ti-662 precluded the formation of beta flecks. It was possible with the 20,000-ton press capacity to extrude at a temperature which was not conducive to beta fleck formation.

As noted in the previous section, the direct aging response of the Ti-8823 alloy was excellent. Unlike the STA heat treatment, uniform strength and toughness values were obtained through-the-section. Microstructure of the DA materials is shown in Figure 15. As shown in the transmission electron micrograph, Figure 15b, the alpha precipitate shows a fine Widmanstätten morphology such as discussed in Reference 12. This type of microstructure was present throughout the entire wall thickness of the DA extrusion. As with the Beta III metastable beta alloy,¹³ the uniform direct aging response is attributed to a residual dislocation structure that is retained after extrusion.

11. FOPIANO, P. J., and HICKEY, C. F., Jr. *Comparison of the Heat Treatment Responses of Three Commercial Titanium Alloys*. Testing and Evaluation, v. 1, November 1973, p. 514.
12. FEENEY, J. A., and BLACKBURN, M. J. *Effect of Microstructure on the Strength, Toughness, and Stress Corrosion Cracking Susceptibility of Metastable Beta Titanium Alloy (Ti-11.5Mo-6Zr-4.5Sn)*. Met. Trans., v. 1, December 1970, p. 3309.
13. ADAIR, A. M., and ROBERSON, J. A. *The Influence of Thermomechanical Processing on the Structure and Properties of Extruded Beta III Titanium*. Proc. Second Int. Conf. on the Strength of Metals and Alloys, v. 3, p. 932, American Society for Metals, Metals Park, Ohio, 1970.



a. 100X



b. 12,000X

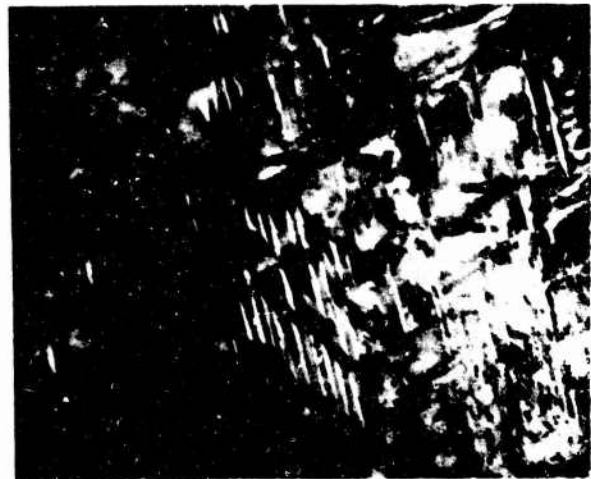
Figure 15. Microstructure of Direct-Aged Ti-8823 at OD Location.
Note Fine Precipitate Shown in Transmission Electron Micrograph (b).

The material that received the STA heat treatment exhibited the lowest strength at the OD as discussed in the previous section. There may be several reasons that could account for this behavior. Bohanek,⁶ working with heavy section forgings of Ti-8823, also observed lower strength levels at the OD and suggested it was due to recrystallization that occurred as a result of lower working temperatures at the OD. In the present effort lower temperatures at the OD of the extrusion were observed. Thermocouples attached to the billet just prior to extrusion showed the temperature to be approximately 1540 F on the skin of the billet after transfer from the 1700 F furnace. As a result, some unrecrystallized regions were observed near the OD as shown in Figure 8. This would indicate that the temperature near the OD was very close to the recrystallization temperature. Subsequent solutionizing at 1475 F probably results in some additional recrystallization. There is a loss of dislocation structure upon recrystallization which reduces the ability to produce a fine network of precipitated alpha during aging.¹³ The microstructure of the material receiving the STA heat treatment is shown in Figure 16a. Note the rather large alpha particles compared to the DA material (Figure 15b). A similar observation was made at the OD and MW of a solid 3-in.-diameter round that received approximately 85% reduction during extrusion. As shown in Figure 17, the coarse alpha precipitation exists near the OD, while at the MW the precipitation is much finer. Whether or not other factors such as time at the solutionizing temperature and cooling rate from the solutionizing temperature have an effect on strength has not been determined. It is perhaps a worthwhile area for future research.

Additional aging time for STA material at the OD can compensate for the effects noted above. A tension specimen from the OD of the STA material was available and given an additional 8-hour aging time. The microstructure of the STA material (16 hours aging cycle) is shown in Figure 16b. As a result of the longer aging time, there was a marked improvement in the strength properties. The σ_{ys} values increased from 168.9 to 175.5 ksi and σ_{uts} values from 181.6 to 186.8 ksi. The σ_{uts} of the STA material (16 hours aging cycle) is less than that of DA material due to a difference in strain hardening capabilities.



a. 1000 F - 8 hr aging time

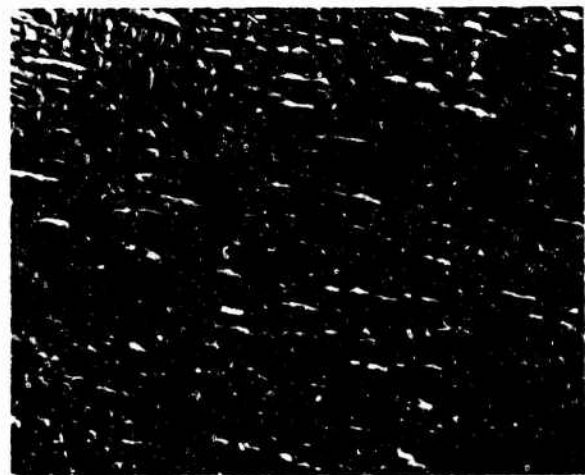


b. 1000 F - 16 hr aging time

Figure 16. Transmission Electron Micrograph of Microstructure of STA Material at the OD. Mag. 12,000X



OD



MW

Figure 17. SEM of Microstructure of 3-in. Extruded Round Given STA Heat Treatment. Mag. 10,000X

As a result of the additional aging time at 1000 F for the STA material, not only did the strength increase but the ductility values were enhanced as well. The reduction of area increased from 5.1% to 9.6% while the elongation increased from 4.0% to 5.0%. These ductility values are closer to those achieved for the DA material. Examination of the cross section of a tension specimen given the original STA heat treatment provides some insight as to reasons behind the lower reduction of area values that were observed. As shown in Figure 18, grain boundary crack initiation is evident. The cracks are more numerous near the fracture surface where the largest values of plastic strain are obtained due to the tensile instability (necking) phenomenon. Closer examination with the SEM reveals formation of the grain boundary cracks via a void formation and growth process as shown in Figure 19. The cross section of the DA tension specimen also revealed some

grain boundary crack initiation; however, the cracks were smaller and less numerous than those observed in the STA material. In any event, the observations of grain boundary crack initiation in both STA and DA materials appear to account for the dependency of ductility on grain size as noted by other investigators.²⁻⁴ With larger grain size material, such as shown in Figure 20, a crack that initiates in a grain boundary has the chance of extending to a larger size for a given amount of deformation before its growth is affected by the intersection with another grain boundary. Hence, with equivalent microstructures the critical crack size is reached and fracture occurs after a smaller amount of deformation than with smaller grain size material.

The stronger tendency for grain boundary crack initiation in the STA material is related to the microstructure in the vicinity of the grain boundary. The microstructure is shown in Figure 21. Note the rather coarse alpha precipitates growing out from the grain boundary. Knoop hardness (KHN) readings were taken with a 100-gram load in the grain boundary region of STA material. These averaged KHN 337, while at the grain interiors KHN averaged 367. With the lower hardness, void initiation and growth occurs earlier in the grain boundary region under tensile deformation, as shown in Figure 18. The microstructure at the grain boundaries also affects rapid crack growth. Examination of the fracture surfaces of fracture toughness specimens reveal a significant difference in the mode of fracture between STA and DA material, as shown in Figure 22. Note the tendency for intergranular fracture in the STA material. The strong tendency of the STA material to exhibit grain boundary crack initiation as well as intergranular crack propagation accounts for the lower fracture toughness and stress corrosion resistance of the STA material when compared to that of the DA material.

How the properties discussed above interact to affect the fatigue behavior is being investigated since it is imperative that any trade-offs include the fatigue properties when weighing one alloy and/or heat treatment against another.

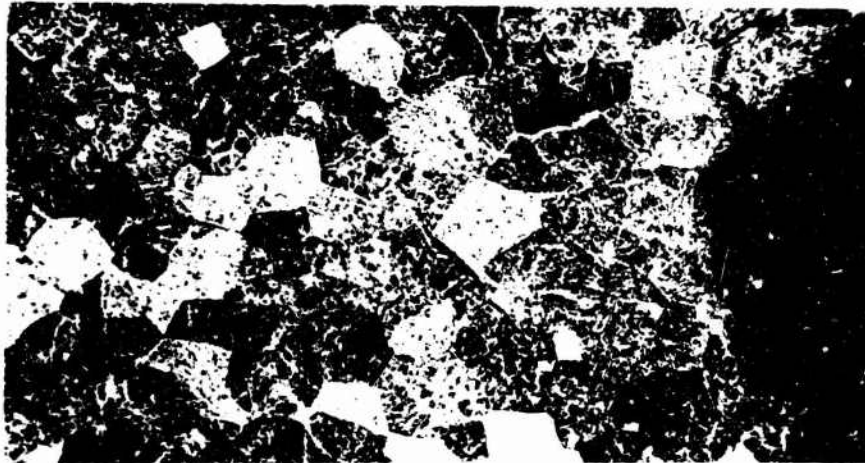
SUMMARY AND CONCLUSIONS

This study has shown that advanced high-strength titanium alloys can be fabricated in large sections by extrusion techniques that provide substantial amounts of hot working. Mechanical properties of such an extrusion of the alpha-beta alloy Ti-662 and the metastable beta alloy Ti-8823 were obtained and, together with microstructural considerations, provide the basis for the following conclusions.

A. Ti-662

1. It is possible to extrude large sections of Ti-662 at temperatures that do not promote "beta fleck" formation.

2. Fracture toughness and ductility of material receiving the STOA heat treatment was excellent. However, these properties were achieved at the expense of about a 20% loss in strength.



Fracture
Surface

Figure 18. Cross Section of Ti-8823 (STA) Tension Specimen Showing Grain Boundary Crack Initiation. Mag. 100X

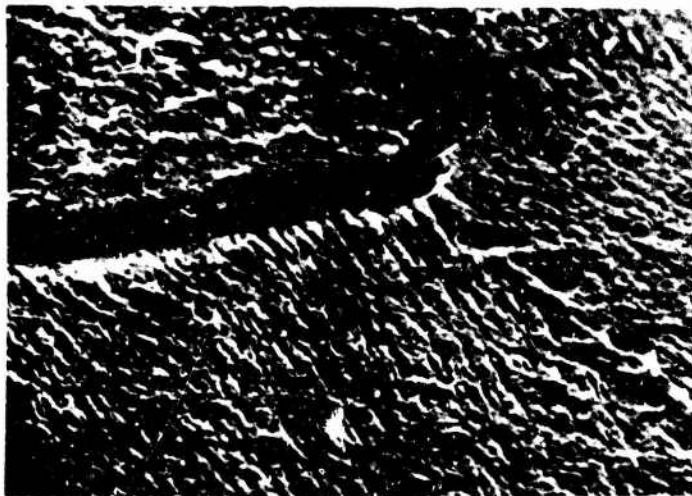


Figure 19. Crack Initiation in Grain Boundary Showing Void Coalescence and Growth Process. Mag. 4000X



a

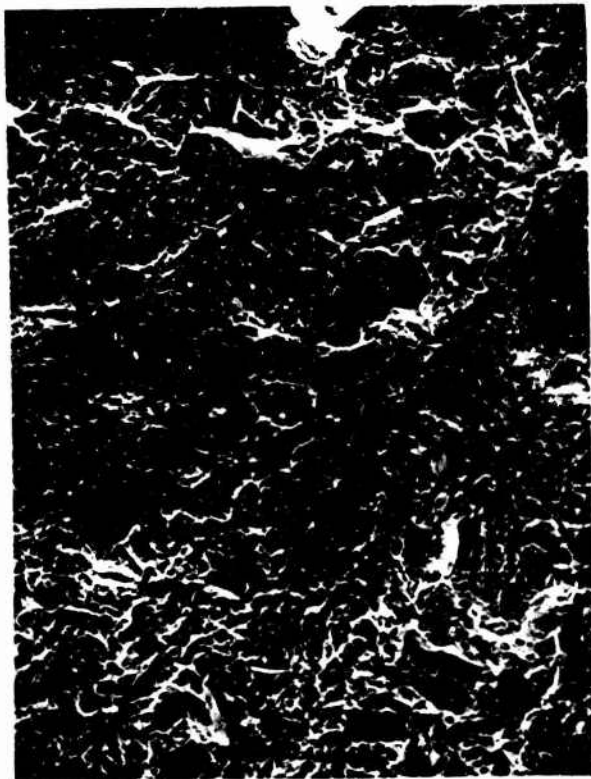


b

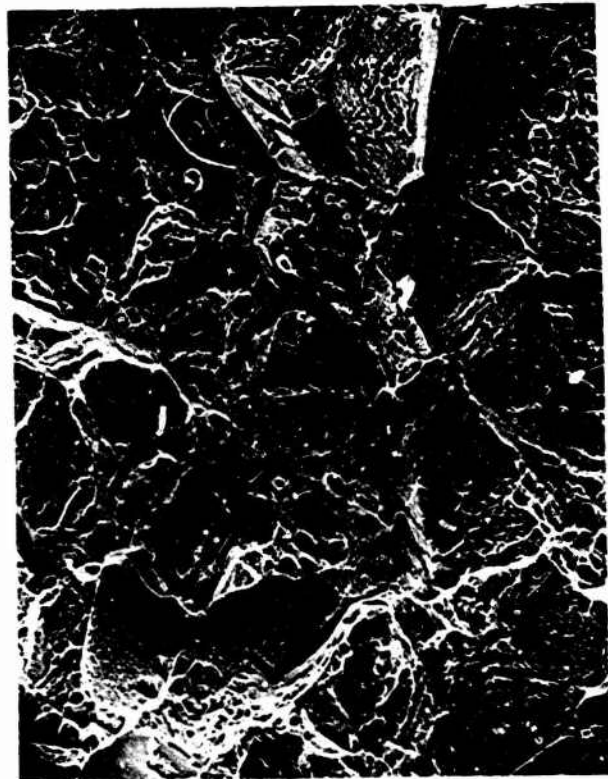
Figure 20. Heat-Treated Microstructures of Material Receiving (a) 84% Reduction and (b) 30% Reduction During Extrusion. Mag. 80X
19-066-1175/AMC-74



Figure 21. Microstructure of the STA Material in the Vicinity of the Grain Boundary. Mag. 12.000X



a. DA Specimen, Mag. 210X



b. STA Specimen, Mag. 110X

Figure 22. Fracture Surfaces of Fracture Toughness Specimens.

B. Ti-8823

1. Direct aging of the extruded product provides uniform through-the-thickness strength behavior.

2. The strength at the OD of the solution treated and aged (STA) material was lower than expected. It is suggested that this is due mainly to a lower working temperature near the OD. A partially recrystallized microstructure near the OD indicates that this temperature was very close to the recrystallization temperature. Subsequent solutionizing at 1475 F probably spurs some additional recrystallization and results in a loss of dislocation structure which reduces the ability to respond to aging.

3. Examination of some tensile fractures indicated a strong tendency for grain boundary crack initiation. This would account for the dependency of ductility on grain size that has been characteristic of metastable beta titanium alloys. Large alpha precipitate near the grain boundaries of the STA material leads to a greater tendency for the initiation of cracks and hence to lower ductility values when compared to DA material.

4. The advantage of direct aging is also evident when fracture toughness and stress corrosion resistance are examined. The STA material tends to exhibit not only grain boundary crack initiation but intergranular crack propagation that accounts for this behavior.